Robust Optimal Sizing of Energy Storage Systems for Dynamic Security of a Grid

Bhagyashree Umathe, Joseph Moyalan, Hyungjin Choi, and Umesh Vaidya

***Abstract*—Battery energy storage systems are becoming prominent for enhancing the resilience of power systems, especially with the increasing penetration of inverter-based resources. This work addresses the robust optimal battery sizing problem by formulating it as a differential game optimal control problem, where minimum control efforts associated with battery capacity are determined under the worst-case disturbance scenarios. To improve scalability, we employ control barrier functions as an alternative to Hamilton-Jacobi-Isaacs equations, enabling computationally efficient solutions to the control problem. The proposed approach generates optimal control trajectories that satisfy dynamic security constraints, providing a robust and scalable framework for identifying feasible battery power and energy capacities that enhance both reliability and economic viability of BESS. Simulation results validate the effectiveness of the method by estimating the optimal rated capacity of BESS in a microgrid with random disturbance in power generation.**

I. Introduction

Battery energy storage systems (BESSs), particularly when integrated with advanced inverter control technologies, are increasingly recognized as vital components for enhancing the resilience of power systems. This significance is amplified by the growing penetration of inverter-based resources (IBRs), which introduce low inertia and uncertainty into the system [1], [2]. To fully harness the potential of BESS, optimal battery sizing that considers dynamic security in uncertain operating conditions is essential, as it enhances the economic viability of investments aimed at strengthening grid resilience.

This work addresses the robust optimal battery sizing problem by integrating dynamic security and the uncertain disturbances inherent in the grid, ultimately providing a solution that enhances both the reliability and economic feasibility of BESS. Our approach formulates this challenge as a min-max optimization control problem, where the inner maximization seeks to amplify the impact of disturbances capturing worst-case scenarios, while the outer minimization focuses on reducing control efforts associated with the installation and operational costs of BESS. Consequently, the solution to this problem yields a minimum battery size that is economically viable and effectively stabilizes the system under the most severe disturbance scenarios.

The problem outlined above is closely tied to resource adequacy planning, where grid resources must be effectively allocated to consistently meet demands, even in the face of severe disturbances. The primary challenge in achieving such a goal stems from the intricate nature of power system models, further complicated by the stochasticity of disturbances within the system. While some studies focus solely on economic factors without considering grid dynamics [3]–[5], many existing works that address dynamic security constraints still tend to oversimplify the system model under deterministic disturbance conditions [6], [7], rendering their findings impractical for real-world applications. In contrast, some research employing meta-heuristic approaches alongside time-domain simulations facilitates a more flexible integration of detailed dynamic components [8]–[10]. However, these methods are often computationally intensive and struggle to effectively manage stochastic disturbances. Similarly, stochastic optimization techniques designed to handle uncertainties are marked by high computational complexity and frequently require a priori knowledge of historical probability distributions, which is not always readily available [11], [12].

The primary contribution of this research is the determination of the minimum control effort, specifically, the battery rated capacity required to meet dynamic security constraints, necessary to manage disturbances from the grid, which are modeled as uncertain variables. Our work presents three significant advancements to the state-of-the-art in this field:

- We address the robust optimal battery sizing problem using a differential game optimal control problem (DGOCP) framework. This method enables us to determine the rated battery capacity needed to meet transient stability constraints under worst-case disturbance scenarios.
- We utilize a control barrier function (CBF) approach [13] to enhance scalability in addressing the DGOCP, providing a practical alternative to the Hamilton-Jacobi-Isaacs (HJI) equations [14], [15]. The HJI equations involve complex partial differential equations (PDEs) that encounter difficulties stemming from the curse of dimensionality in large-scale systems [15].
- Furthermore, we integrate the Koopman operator modeling approach to exploit linearity, enabling explicit optimal solutions to the DGOCP and significantly reducing computational overhead.
- Our approach produces an optimal control trajectory for BESS responses under worst-case disturbances while satisfying dynamic security constraints, enabling us to estimate the minimum required rated energy capacity.

Consequently, our proposed approach determines the minimum power and energy capacities needed for BESSs to satisfy stability criteria across all potential disturbance scenarios.

The remainder of the paper is organized as follows. In

Bhagyashree Umathe, Joseph Moyalan and Umesh Vaidya are with the Department of Mechanical Engineering, Clemson University, Clemson, SC, ({bumathe,jmoyala,uvaidya}@clemson.edu). Hyungjin Choi is with Sandia National Laboratories, Albuquerque, NM (hchoi@sandia.gov)

979-8-3315-8138-1

Section II, we introduce the formulation of robust optimal battery sizing within the context of uncertain power systems, leveraging the DGOCP framework. This section highlights the main contribution of the paper, which focuses on safe control design using the control barrier function method. Section III presents simulation results in a microgrid setting, considering disturbances in power generation. Finally, conclusions and directions for future work are discussed in Section IV.

II. Optimal Battery Sizing via Differential Game Optimal Control

In this section, we present a novel framework for optimal battery sizing grounded in the differential game optimal control problem. The central concept involves the integration of control barrier functions with Koopman operator models. This approach facilitates computationally efficient optimal solutions to the DGOCP while simultaneously addressing both cost minimization and stability assurance.

A. Formulation of Optimal Battery Sizing as Differential Game Optimal Control Problem

The electromechanical dynamics of power systems are commonly modeled using differential-algebraic equations (DAEs), expressed as follows:

$$\dot{\mathbf{x}} = \mathbf{f}(\mathbf{x}, \mathbf{y}, \mathbf{u}, \mathbf{d}),\ \mathbf{0} = \mathbf{g}(\mathbf{x}, \mathbf{y}, \mathbf{u}, \mathbf{d}), \tag{1}$$

where $\mathbf{x} \in \mathbb{R}^n$ represents dynamic states (e.g., generator speeds and angles), and $\mathbf{y} \in \mathbb{R}^p$ denotes algebraic states (e.g., bus voltages and angles). The control input $\mathbf{u} \in \mathbb{R}^m$ corresponds to the battery output power, while $\mathbf{d} \in \mathbb{R}^q$ captures uncertain operating conditions such as variable generation, load demand, or unexpected faults.

Within this modeling framework, the optimal battery sizing problem, ensuring dynamic security of the power system, can be formulated as a DGOCP as follows:

$$\min_{\mathbf{u}} \max_{\mathbf{d}} \int_0^{t_f} L(\mathbf{x}, \mathbf{y}, \mathbf{u}, \mathbf{d})\, dt \tag{2a}$$

$$\text{s.t.}\quad \dot{\mathbf{x}} = \mathbf{f}(\mathbf{x}, \mathbf{y}, \mathbf{u}, \mathbf{d}),\ \mathbf{0} = \mathbf{g}(\mathbf{x}, \mathbf{y}, \mathbf{u}, \mathbf{d}), \tag{2b}$$

$$\mathbf{x}, \mathbf{y} \in \mathcal{S},\ \mathbf{u} \in \mathcal{U}, \mathbf{d} \in \mathcal{D}. \tag{2c}$$

Here, L represents the objective function that minimizes battery capacity. The set $\mathcal{S}$ defines security constraints to ensure stable system operation, while $\mathcal{U}$ and $\mathcal{D}$ specify feasible ranges for battery power and disturbance scenarios, respectively.

The inner maximization problem in(2a) aims to identify adversarial disturbances $\mathbf{d}$ that most significantly affect system stability by maximizing the cost function with respect to $\mathbf{d}$, which in turn increases the necessary battery capacity to maintain adequate reserves. As a result, the overall optimization problem in (2a)-(2c) seeks to determine the minimum rated power capacity of the battery that robustly ensures stability under worst-case disturbance scenarios.

The safety set $\mathcal{S}$ is defined as:

$$\mathcal{S} := \{[\mathbf{x}^\top, \mathbf{y}^\top]^\top \in \mathbb{R}^{n+p} : \mathbf{h}(\mathbf{x}, \mathbf{y}) \geq 0\} \tag{3}$$

where $\mathbf{h}(\mathbf{x}, \mathbf{y})$ encodes constraints that ensure safe system operation. For example, voltage deviations are typically constrained to $\pm 5\%$ [pu] around unity, while frequency deviations are limited to ± 0.5 Hz. In many cases, the safety set can be represented using interval or box constraints.

Assume unknown but bounded disturbance $\mathbf{d}$ within a set:

$$\mathcal{D} := \{\mathbf{d} \in \mathbb{R}^q : \mathbf{d}_{\min} \leq \mathbf{d} \leq \mathbf{d}_{\max}\} \tag{4}$$

where $\mathbf{d}_{\min}$ and $\mathbf{d}_{\max}$ represent bounds on disturbance variations. This assumption is practical, as it captures realistic scenarios in which the distribution or actual dynamics of disturbances are unknown, yet we possess information about their maximum variations derived from historical data. Similarly, the feasible battery rated power limits are defined as:

$$\mathcal{U} := \{\mathbf{u} \in \mathbb{R}^m : -\mathbf{u}_{\mathrm{r}} \leq \mathbf{u} \leq \mathbf{u}_{\mathrm{r}}\} \tag{5}$$

where $\mathbf{u}_{\mathrm{r}}$ specifies the maximum rated power of the BESS.

Solving the DGOCP in (2) typically involves computationally intensive numerical procedures. In the next section, we present a scalable approach based on control barrier functions to efficiently address this optimization problem.

B. Solutions to DGOCP via Control Barrier Functions

The DGOCP described in the previous section is challenging to solve directly due to the complexity of the HJI equations that arise in differential game formulations [16]. These equations are nonlinear partial differential equations that require spatial discretization and numerical solution techniques, often leading to significant computational overhead - a phenomenon referred to as the curse of dimensionality [15]. To improve scalability, we employ control barrier functions.

Assuming an explicit algebraic relationship $\mathbf{y} = \phi(\mathbf{x}, \mathbf{u}, \mathbf{d})$, a CBF V satisfies the following properties: $V(0) = 0$, $V \geq 0$,

$$\inf_{\mathbf{d} \in \mathcal{D}} |\dot{V}(\mathbf{x})| \geq -\alpha(V(\mathbf{x})) \tag{6}$$

where $\alpha(\cdot)$ is a continuous, strictly increasing function with $\alpha(0) = 0$ (e.g., $\alpha(s) = \gamma s$, $\gamma > 0$), and $\dot{V}$ is expressed as:

$$\dot{V}(\mathbf{x}) = \nabla V(\mathbf{x})^\top \mathbf{f}(\mathbf{x}, \phi(\mathbf{x}, \mathbf{u}, \mathbf{d}), \mathbf{u}, \mathbf{d}). \tag{7}$$

The function V is designed to approximate $\mathbf{h}$ in a simplified form, such as an ellipsoid. The conditions above ensure the forward invariance of the safety set $\mathcal{S}$ under worst-case disturbances $\mathbf{d}$ [13]. In other words, for any control input $\mathbf{u} \in \mathcal{U}$ satisfying these conditions, the state $\mathbf{x} \in \mathcal{S}$ remains within the safety set for all disturbances $\mathbf{d} \in \mathcal{D}$ at all times.

Given the constraint in (6), the original DGOCP in (2) can be reformulated as follows:

$$\min_{\mathbf{u} \in \mathcal{U}} L(\mathbf{x}, \mathbf{y}, \mathbf{u}, \mathbf{d}) \ \text{ s.t. } \inf_{\mathbf{d} \in \mathcal{D}} |\dot{V}(\mathbf{x})| \geq -\alpha(V(\mathbf{x})). \tag{8}$$

This reformulation simplifies the solution process by reducing the problem to a constrained minimization at each time step, rather than synthesizing a closed-form feedback control law for all times t. The minimum battery power and energy capacities, denoted by $\mathbf{P}_{\min}$ and $\mathbf{E}_{\min}$, can then be determined using the maximum control solution across all time steps:

$$\mathbf{P}_{\min} = \max_{t \in [0, t_f]} (\mathbf{u}^\star(t)),\ \mathbf{E}_{\min} = \int_{t=0}^{t_f} \mathbf{u}^\star(t) dt \tag{9}$$

where $\mathbf{u}^\star(t)$ is the optimal solution of (8) at time t.

In the next section, we introduce the Koopman operator approach, which transforms the DAE model into an equivalent linear representation. This transformation facilitates explicit derivation of CBF constraints and efficient computation of solutions to the reformulated optimization problem.

C. Explicit Solutions to DGOCP via Koopman Operators

In this section, we derive optimal solutions to DGOCP by leveraging the Koopman operator modeling approach. The Koopman operator is a mathematical framework that enables a linear representation of nonlinear dynamics, making it particularly advantageous for control and optimization tasks. Data-driven methods, such as the extended dynamic mode decomposition (EDMD), can be employed to estimate the Koopman operator from time-series data, further enhancing its applicability in practical engineering problems. For a detailed exposition on Koopman operator theory and the EDMD algorithm, refer to [17]–[19].

Without loss of generality, the nonlinear DAE model in (1) can be represented in a lifted coordinate space using the Koopman operator as follows:

$$\dot{\Phi}(\mathbf{x}) = \mathbf{A}_\Phi \, \Phi(\mathbf{x}) + \mathbf{B}_u \, \mathbf{u} + \mathbf{B}_d \, \mathbf{d}, \tag{10a}$$

$$\mathbf{y} = \mathbf{C} \, \Phi(\mathbf{x}) + \mathbf{D} \, \mathbf{u}. \tag{10b}$$

In this formulation, disturbances primarily influence the lifted-state dynamics and therefore do not explicitly appear in the algebraic output equation.

where $\Phi(\mathbf{x}) = [\phi_1(\mathbf{x}), \ldots, \phi_N(\mathbf{x})]^\top$ represents a set of basis functions, such as polynomials or radial basis functions (RBFs) [19]. The matrices $\mathbf{A}_\Phi$, $\mathbf{B}_u$, and $\mathbf{B}_d$ define the linear dynamics in the lifted function space for the control input $\mathbf{u}$ and disturbance $\mathbf{d}$, while $\mathbf{C}$ and $\mathbf{D}$ map the lifted state $\Phi(\mathbf{x})$ and inputs $\mathbf{u}$ and $\mathbf{d}$ to the output $\mathbf{y}$. This linear representation provides a computationally efficient reformulation of the original nonlinear DAE model.

To estimate the Koopman model, we approach the problem by solving a series of least-squares optimization tasks utilizing discrete time-series data denoted as $\{\mathbf{x}_k, \mathbf{y}_k, \mathbf{u}_k, \mathbf{d}_k\}_{k=1}^{T}$. In this context, T represents the terminal time of the discrete time interval, characterized by a time step of Δt, i.e., $t_f = T \Delta t$. The optimization problems can be formulated as follows:

$$\min_{\mathbf{G}} \; \textstyle\sum_{k=1}^{T} |\dot{\Phi}(\mathbf{x}_k) - \mathbf{G}\Theta_k|^2 + \lambda \|\mathbf{G}\|^2, \; \lambda > 0 \tag{11}$$

$$\min_{\mathbf{C},\mathbf{D}} \; \textstyle\sum_{k=1}^{T} |\mathbf{y}_k - \mathbf{C}\Phi(\mathbf{x}_k) - \mathbf{D}\mathbf{u}_k|^2 \tag{12}$$

where $\mathbf{G} = [\mathbf{A}_\Phi, \mathbf{B}_u, \mathbf{B}_d]$, $\Theta_k = [\Phi(\mathbf{x}_k)^\top, \mathbf{u}_k^\top, \mathbf{d}_k^\top]^\top$. λ serves as a regularization, effectively penalizing the linear system matrices to enhance robustness to noisy measurement.

Assume the safety set $\mathcal{S}$ is defined on the algebraic variables $\mathbf{y}$ and described by axis-parallel box constraints: $y_i^{\min} \le y_i \le y_i^{\max}$ for $i = 1, \ldots, p$. To approximate $\mathcal{S}$, we introduce a control barrier function (CBF) as an ellipsoidal approximation:

$$V(\mathbf{y}) := \mathbf{y}^\top \mathbf{Q}_1 \mathbf{y} + \mathbf{Q}_2^\top \mathbf{y} + q3, \tag{13}$$

where $\mathbf{Q}_1 = \mathrm{diag}\Big(\frac{1}{r_1^2}, \frac{1}{r_2^2}, \ldots, \frac{1}{r_n^2}\Big)$, $\mathbf{Q}_2 = -2\mathbf{Q}_1\mathbf{y}_c$, $q_3 = \mathbf{y}_c^\top \mathbf{Q}_1 \mathbf{y}_c - 1$. $\mathbf{y}_c = (y_i^{\min} + y_i^{\max})/2$ represents the center of the box, and $\mathbf{y}_r = (y_i^{\max} - y_i^{\min})/2$ defines the radius. The above ellipsoid is the largest contained within the box $\mathcal{S}$.

Substituting the linear algebraic model (10b) into (13), the CBF is expressed as:

$$V = -\left(\mathbf{\Phi}^\top \mathbf{P}_1 \mathbf{\Phi} + \mathbf{p}^\top \mathbf{\Phi} + \mathbf{s}(\mathbf{x})^\top \mathbf{u} + \mathbf{u}^\top \mathbf{P}_2 \mathbf{u} + q_3\right) \tag{14}$$

where $\mathbf{s}(\mathbf{x}) := 2\,\mathbf{P}_3^\top \mathbf{\Phi}$, $\mathbf{P}_1 = \mathbf{C}^\top \mathbf{Q}_1 \mathbf{C}$, $\mathbf{P}_3 = \mathbf{C}^\top \mathbf{Q}_1 \mathbf{D}$, $\mathbf{P}_2 = \mathbf{D}^\top \mathbf{Q}_1 \mathbf{D}$, $\mathbf{p} = \mathbf{C}^\top \mathbf{Q}_2$, and q_3 is constant; $\mathbf{C}$ and $\mathbf{D}$ denote the lifted-state and input coefficient matrices, respectively. To obtain a control-independent barrier function, we bound the linear and quadratic input terms in V over the admissible set $\mathcal{U}$. Using $\max_{\mathbf{u}\in\mathcal{U}} \mathbf{s}(\mathbf{x})^\top \mathbf{u} = |\mathbf{s}(\mathbf{x})|^\top \mathbf{u}^{\max}$ and $\max_{\mathbf{u}\in\mathcal{U}} \mathbf{u}^\top \mathbf{P}_2 \mathbf{u} \le (\mathbf{u}^{\max})^\top |\mathbf{P}_2| \, \mathbf{u}^{\max}$, the resulting input-independent barrier function is

$$\begin{aligned} \hat{V}(\mathbf{x}) = -(&\mathbf{\Phi}^\top \mathbf{P}_1 \mathbf{\Phi} + \mathbf{p}^\top \mathbf{\Phi} + |\mathbf{s}(\mathbf{x})|^\top \mathbf{u}^{\max} \\ &+ (\mathbf{u}^{\max})^\top |\mathbf{P}_2| \, \mathbf{u}^{\max} + q_3), \end{aligned} \tag{15}$$

where $|\cdot|$ denotes elementwise absolute value and $\mathbf{u}^{\max}$ collects the componentwise bounds on $\mathbf{u}$. This satisfies $V(\mathbf{x}, \mathbf{u}) \ge \hat{V}(\mathbf{x})$ for all $\mathbf{u} \in \mathcal{U}$.

Since the Koopman model in (10) is affine in $\mathbf{d}$, the disturbance appears in the CBF condition only through the linear term $\nabla \hat{V}^\top \mathbf{B}_d \mathbf{d}$. Maximizing this term over the admissible disturbance set $\mathcal{D}$ yields

$$\mathbf{d}_{\max} = \hat{\mathbf{d}} \odot \mathrm{sgn}\Big(\mathbf{B}_d^\top \nabla \hat{V}\Big), \tag{16}$$

where $\hat{\mathbf{d}}$ collects the componentwise disturbance bounds and $\odot$ denotes elementwise multiplication.

Applying the CBF condition in (6) to the Koopman model (10), together with $\hat{V}$ in (15) and the worst-case disturbance (16), leads to the following linear inequality in $\mathbf{u}$:

$$-\nabla \hat{V}^\top \mathbf{B}_u \mathbf{u} \;\le\; \nabla \hat{V}^\top (\mathbf{A}_\Phi \mathbf{\Phi} + \mathbf{B}_d \mathbf{d}_{\max}) + \gamma \hat{V}. \tag{17}$$

The control input is then obtained at each time step by solving

$$\min_{\mathbf{u}\in\mathcal{U}} \; \frac{1}{2} \mathbf{u}^\top \mathbf{H} \mathbf{u} \tag{18a}$$

$$\text{s.t.} \; -\nabla \hat{V}^\top \mathbf{B}_u \mathbf{u} \le \nabla \hat{V}^\top (\mathbf{A}_\Phi \mathbf{\Phi} + \mathbf{B}_d \mathbf{d}_{\max}) + \gamma \hat{V}, \tag{18b}$$

where $\mathbf{H} \succ 0$ weights the control effort. The problem in (15) can be computationally intensive to solve directly. To mitigate this complexity, we evaluate $\tilde{V}$ for various values of $\mathbf{u} \in (0, \mathbf{u}_\mathrm{r}]$ and iteratively solve the QP in (18) for the corresponding $\tilde{V}$. The optimal solution $\mathbf{u}_{i,k}^\star$ from the i-th iteration at time step k is used to estimate the minimum battery power and energy, $\mathbf{u}_{\text{min},i}$ and $\mathbf{E}_{\text{min},i}$, required to maintain the safety set:

$$\mathbf{u}_{\text{min},i} = \max\left(\mathbf{u}_{i,k}^\star\right), \; \mathbf{E}_{\text{min},i} = \max\left(\sum_{t=0}^{T} \mathbf{u}_{i,k}^\star \Delta t\right) \tag{19}$$

for $k = 1, \ldots, T$. This process is repeated M times to evaluate $\tilde{V}$ for different $\mathbf{u}$. The final battery size is selected as the maximum control effort observed across all M simulations:

$$\mathbf{P}_{\text{min}} := \max_{i=1,\ldots,M} (\mathbf{u}_{\text{min},i}), \; \mathbf{E}_{\text{min}} := \max_{i=1,\ldots,M} (\mathbf{E}_{\text{min},i}). \tag{20}$$

This simulation-driven CBF-QP framework provides a conservative and efficient method for estimating the minimum

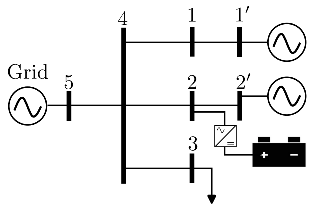

Fig. 1: Test power system in this numerical demonstration.

battery rating needed to keep system states within the safety set under worst-case disturbances. A key benefit of addressing (18) is its deterministic evaluation of the robust optimal battery sizing problem in (2), which simplifies the complexity of the HJI equations as the dimensions of $\mathcal{U}$ and $\mathcal{D}$ increase.

III. Simulation Results

In this section, we demonstrate the proposed method for estimating the optimal battery capacity to enhance grid stability for the test case illustrated in Fig. 1.

A. Power System Models

The dynamics of the test case are described as below.

1) Synchronous Generator at bus $1'$*:*

$$\dot{\delta}_1 = \omega_1 - \omega_s, \tag{21a}$$

$$M_1\dot{\omega}_1 = P_1 - \frac{E_1 V_1}{X_1'}\sin(\delta_1 - \theta_1) - D_1(\omega_1 - \omega_s), \tag{21b}$$

$$T_1^0 \dot{E}_1 = E_1^f - \frac{X_1}{X_1'}E_1 + \frac{X_1 - X_1'}{X_1'}V_1\cos(\delta_1 - \theta_1), \tag{21c}$$

where M_1 and D_1 are the inertia and damping constants; P_1 and E_1 represent the generator power and voltage; T_1^0 is the excitor time constant; X_1 and X_1' denote the flux and transient reactances; V_1 and θ_1 are the voltage magnitude and angle at the generator bus; and ω_s is the system frequency.

2) Doubly Fed Induction Generator (DFIG) at bus $2'$*:*

$$\begin{aligned}\dot{\delta}_2 = \frac{1}{T_2^0 E_2}\Big[& - T_2^0(\omega_s - \omega_2)E_2 - \bar{X}_2 V_2 \sin(\delta_2 - \theta_2) \\ & + T_2^0 \omega_s V_2^r \cos(\delta_2 - \theta_2^r)\Big],\end{aligned} \tag{22a}$$

$$\dot{\omega}_2 = \frac{1}{M_2}\Big[\frac{\omega_s}{\omega_2}P_2 - \frac{E_2 V_2}{X_2'}\sin(\delta_2 - \theta_2)\Big], \tag{22b}$$

$$\begin{aligned}\dot{E}_2 = \frac{1}{T_2^0}\Big[& - \frac{X_2}{\bar{X}_2'}E_2 + \frac{X_2 - X_2'}{X_2'}V_2\cos(\delta_2 - \theta_2) \\ & + \omega_s V_2^r \sin(\delta_2 - \theta_2^r)\Big],\end{aligned} \tag{22c}$$

where T_2^0 is the generator time constant; X_2 and X_2' are the flux and transient reactances; E_2 and P_2 represent the generator field voltage and power; and V_2 and θ_2^r are the rotor voltage magnitude and angle, assuming constant in this study.

3) Power flow equations:

$$P_L^i = -G_{ii}V_i^2 + \sum_{j\in\mathcal{N}_i} V_i V_j (G_{ij}\cos\theta_{ij} + B_{ij}\sin\theta_{ij}), \tag{23a}$$

$$Q_L^i = B_{ii}V_i^2 + \sum_{j\in\mathcal{N}_i} V_i V_j (G_{ij}\sin\theta_{ij} - B_{ij}\cos\theta_{ij}), \tag{23b}$$

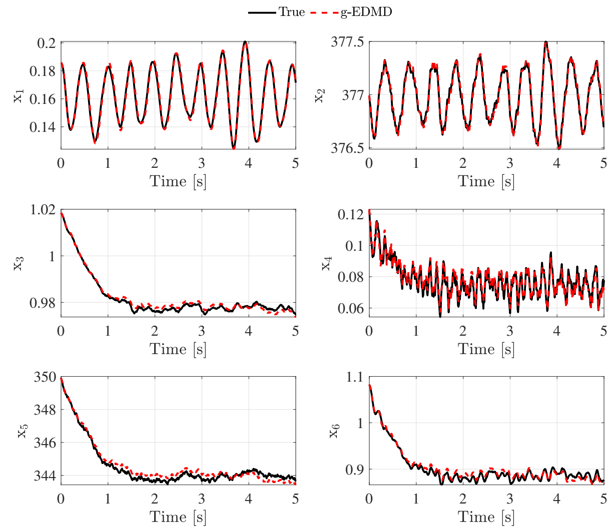

Fig. 2: The Koopman model accuracy is validated by comparing trajectories with those from the original DAE model.

where G_{ij} and B_{ij} are the line admittance and susceptance between bus i and j; $\mathcal{N}_i$ is the set of buses electrically connected to bus i; $\theta_{ij} = \theta_i - \theta_j$ denotes the angle difference between buses i and j; and P_i^L and Q_i^L are active and reactive power of the load at bus i ($P_i^L = 0$, $Q_i^L = 0$, $\forall i \notin \{3\}$).

4) Control Inputs and Disturbances: Output power of the BESS at bus 2 is modeled as an active power injection to the bus. Thus, the active power balance at bus 2 includes the control input $u = P^{\mathrm{BESS}}$, expressed as:

$$\begin{aligned}0 = {} & G_{22}V_2^2 - V_2 V_{2'}(G_{22'}\cos\theta_{22'} + B_{22'}\sin\theta_{22'}) \\ & - V_2 V_4 (G_{24}\cos\theta_{24} + B_{24}\sin\theta_{24}) + u\end{aligned} \tag{24}$$

For disturbance scenario, we consider uncertainty in the active power of the generator at bus 2, denoted as $d = P_2$. The uncertainty is modeled as unknown-but-bounded, with 30 [%] variations around the nominal value $\bar{P}_2 = 0.07$ [pu], i.e.,

$$0.7\bar{P}_2 \le d \le 1.3\bar{P}_2 \ [\mathrm{pu}]. \tag{25}$$

B. Estimation of Koopman Operator Model

In this work, we construct linear system models equivalent to the original power system dynamics, following the proposed method in Section II-C. We collect approximately 50,000 time-series data points from repeated simulations of the dynamical model in (21)–(24) with $\mathbf{x} = [\delta_1, \omega_1, E_1, \delta_2, \omega_2, E_2]^\top$, and $\mathbf{y} = [V_1, \theta_1, V_2, \theta_2, V_3, \theta_3, V_4, \theta_4]^\top$, performed with $\Delta t = 0.01$ [s], starting from random initial conditions for $u \in [-0.1, 0.1]$ [pu] and $d \in [0.05, 0.09]$ [pu]. We then use this dataset to construct a linear model in (10), utilizing second-order polynomial basis functions in transformed coordinates. The model's fidelity is evaluated by comparing the simulated trajectories from the original DAE model with those from the Koopman operator model, as depicted in Fig. 2.

C. Solutions to Optimal Battery Size via DGOCP Framework

We employ the DGOCP framework outlined in Section II by imposing safety limits on the bus voltage magnitudes,

$$\mathcal{S} = \{V_i,\, i = 1, \ldots, 5 \,:\, 0.95 \le V_i \le 1.05 \ [\mathrm{pu}]\}\,. \tag{26}$$

979-8-3315-8138-1

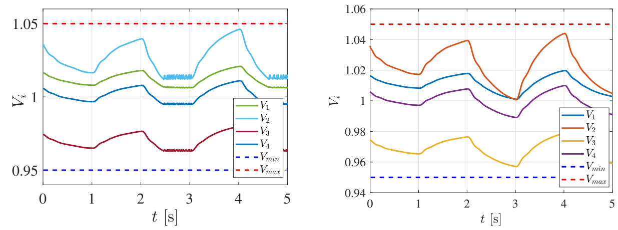

(a) (b)

Fig. 3: Voltage trajectories under a random disturbance using QP-CBF control: Koopman model and nonlinear DAE model.

To ensure these safety limits, we construct an ellipsoidal CBF within $\mathcal{S}$ with conservative control direction, as detailed in (15), leading us to formulate the QP problem in (18). At each time k, we solve the QP problem in (18) over a finite time interval of $t_f = 5$ [s] to obtain the optimal control $u^\star_{i,k}(t)$ using the estimated Koopman model, taking into account the time steps in real-time operations. Without loss of generality, the method is applicable for longer control time horizon for t_f as required by a specific application. We perform $N = 100$ iterations to evaluate the CBF $\tilde{V}$ with $\mathbf{u} \in [0, 0.1]$. From the QP solutions, we estimate the minimum rated battery power and energy based on (19)–(20), yielding $P_{\min} = 50$ [MW] and $E_{\min} = 150$ [MWh], while ensuring compliance with the safe operating limits on bus voltages. We verify that bus voltage magnitudes remain within the safe set across multiple simulations with varying disturbances, as shown in Fig. 3b.

IV. Conclusions

We proposed a comprehensive method to evaluate rated capacity of BESS for effectively managing grid disturbances. By employing the CBF method, we successfully identify the worst-case disturbances and the corresponding optimal battery responses, which allows us to accurately determine the necessary battery capacity to ensure voltage safety across the grid. The integration of a linear control strategy with the Koopman operator significantly enhances the performance of our method, enabling more precise control over battery operations for grid stability acknowledging worst-case disturbances. Looking ahead, we plan to extend this framework to incorporate inverter and battery dynamics, which will further improve its applicability and robustness in large-scale power systems. This advancement will not only contribute to the reliability of grid operations but also support the transition towards inverter-dominant power systems.

V. Acknowledgement

Financial support from NSF 2031573 is greatly acknowledged. Also, this material is based upon work supported by the U.S. Department of Energy, Office of Electricity (OE), Energy Storage Division. This article has been authored by an employee of National Technology & Engineering Solutions of Sandia, LLC under Contract No. DE-NA0003525 with the U.S. Department of Energy (DOE). The employee owns all right, title and interest in and to the article and is solely responsible for its contents. The United States Government retains and the publisher, by accepting the article for publication, acknowledges that the United States Government retains a non-exclusive, paid-up, irrevocable, world-wide license to publish or reproduce the published form of this article or allow others to do so, for United States Government purposes. The DOE will provide public access to these results of federally sponsored research in accordance with the DOE Public Access Plan https://www.energy.gov/downloads/doe-public-access-plan.

References

[1] A. Ulbig, T. Borsche, and G. Andersson, "Impact of low rotational inertia on power system stability and operation," *IFAC Proceedings Volumes*, vol. 47, no. 3, pp. 7290–7297, 2014, 19th IFAC World Congress.

[2] M. Shadoul, R. Ahshan, R. S. AlAbri, A. Al-Badi, M. Albadi, and M. Jamil, "A comprehensive review on a virtual-synchronous generator: Topologies, control orders and techniques, energy storages, and applications," *Energies*, vol. 15, no. 22, p. 8406, November 2022.

[3] A. Alanazi, H. Lotfi, and A. Khodaei, "Optimal energy storage sizing and siting in hybrid ac/dc microgrids," in *2018 North American Power Symposium (NAPS)*, 2018, pp. 1–6.

[4] X. Wu, J. Zhao, and A. J. Conejo, "Optimal battery sizing for frequency regulation and energy arbitrage," *IEEE Transactions on Power Delivery*, vol. 37, no. 3, pp. 2016–2023, 2022.

[5] T. A. Nguyen, M. L. Crow, and A. C. Elmore, "Optimal sizing of a vanadium redox battery system for microgrid systems," *IEEE Transactions on Sustainable Energy*, vol. 6, no. 3, pp. 729–737, 2015.

[6] M. Javadi, Y. Gong, and C. Y. Chung, "Frequency stability constrained bess sizing model for microgrids," *IEEE Transactions on Power Systems*, vol. 39, no. 2, pp. 2866–2878, 2024.

[7] S. Bahramirad, W. Reder, and A. Khodaei, "Reliability-constrained optimal sizing of energy storage system in a microgrid," *IEEE Transactions on Smart Grid*, vol. 3, no. 4, pp. 2056–2062, 2012.

[8] D. Zhang, G. Shafiullah, C. K. Das, and K. W. Wong, "Optimal allocation of battery energy storage systems to improve system reliability and voltage and frequency stability in weak grids," *Applied Energy*, vol. 377, p. 124541, 2025.

[9] N.-C. Yang, Y.-C. Zhang, and E. W. Adinda, "Sizing and sitting of battery energy storage systems in distribution networks with transient stability consideration," *Mathematics*, vol. 10, no. 19, p. 3420, Sep. 2022.

[10] K. S. El-Bidairi, H. D. Nguyen, T. S. Mahmoud, S. Jayasinghe, and J. M. Guerrero, "Optimal sizing of battery energy storage systems for dynamic frequency control in an islanded microgrid: A case study of flinders island, australia," *Energy*, vol. 195, p. 117059, 2020.

[11] D. Zhang, J. Li, X. Liu, J. Guo, and S. Xu, "A stochastic optimization method for energy storage sizing based on an expected value model," *Energies*, vol. 12, no. 4, p. 702, Feb. 2019.

[12] X. Xi, R. Sioshansi, and V. Marano, "A stochastic dynamic programming model for co-optimization of distributed energy storage," *Energy Systems*, vol. 5, no. 3, p. 475–505, Nov. 2013.

[13] A. D. Ames, S. Coogan, M. Egerstedt, G. Notomista, K. Sreenath, and P. Tabuada, "Control barrier functions: Theory and applications," in *2019 18th European Control Conference (ECC)*, 2019, pp. 3420–3431.

[14] H. V. Tran, *Hamilton-Jacobi equations*, ser. Graduate Studies in Mathematics. Providence, RI: American Mathematical Society, Jan. 2022.

[15] I. M. Mitchell, A. M. Bayen, and C. J. Tomlin, "A time-dependent hamilton-jacobi formulation of reachable sets for continuous dynamic games," *IEEE Transactions on automatic control*, vol. 50, no. 7, pp. 947–957, 2005.

[16] T. Başar and G. J. Olsder, *Dynamic noncooperative game theory, 2nd edition*. Society for Industrial and Applied Mathematics, Jan. 1998.

[17] A. Lasota and M. C. Mackey, *Chaos, Fractals, and Noise: Stochastic Aspects of Dynamics*. New York: Springer-Verlag, 1994.

[18] I. Mezić, "Spectral properties of dynamical systems, model reduction and decompositions," *Nonlinear Dynamics*, vol. 41, no. 1-3, pp. 309–325, 2005.

[19] M. O. Williams, I. G. Kevrekidis, and C. W. Rowley, "A data–driven approximation of the koopman operator: Extending dynamic mode decomposition," *Journal of Nonlinear Science*, vol. 25, no. 6, p. 1307–1346, Jun. 2015.

979-8-3315-8138-1